Effect of applied toroidal electric field on the growth/decay of plateau-phase runaway electron currents in DIII-D

2011 Nucl. Fusion 51 103026

(http://iopscience.iop.org/0029-5515/51/10/103026)

IOP Publishing and International Atomic Energy Agency Nuclear Fusion
Nucl. Fusion **51** (2011) 103026 (8pp) doi:10.1088/0029-5515/51/10/103026

Effect of applied toroidal electric field on the growth/decay of plateau-phase runaway electron currents in DIII-D

E.M. Hollmann[1], P.B. Parks[2], D.A. Humphreys[2], N.H. Brooks[2], N. Commaux[3], N. Eidietis[2], T.E. Evans[2], R. Isler[3], A.N. James[1], T.C. Jernigan[3], J. Munoz[4], E.J. Strait[2], C. Tsui[5], J. Wesley[2] and J.H. Yu[1]

[1] Center for Energy Research, University of California–San Diego, San Diego, CA, USA
[2] General Atomics, PO Box 85608, San Diego, CA, USA
[3] Oak Ridge National Laboratory, Oak Ridge, TN, USA
[4] Oak Ridge Associated Universities, Oak Ridge, TN, USA
[5] Institute for Aerospace Studies, University of Toronto, Toronto, Canada

Received 12 May 2011, accepted for publication 9 August 2011
Published 2 September 2011
Online at stacks.iop.org/NF/51/103026

Abstract
Large relativistic runaway electron currents (0.1–0.5 MA) persisting for ~100 ms are created in the DIII-D tokamak during rapid discharge shut down caused by argon pellet injection. Slow upward and downward ramps in runaway currents were found in response to externally applied loop voltages. Comparison between the observed current growth/decay rate and the rate expected from the knock-on avalanche mechanism suggests that classical collisional dissipation of runaways alone cannot account for the measured growth/damping rates. It appears that a fairly constant anomalous dissipation rate of order $10\,s^{-1}$ exists, possibly stemming from radial transport or direct orbit losses to the vessel walls, although the possibility of an apparent loss due to current profile shrinking cannot be ruled out at present.

(Some figures in this article are in colour only in the electronic version)

1. Introduction

Runaway electrons (REs) are observed to form in tokamaks when large toroidal electric fields are present—typically during startup, periods of strong radio-frequency current drive, or during the current quench (CQ) of disruptions. In disruptions, a variety of processes are thought to generate RE seeds [1–3]. These RE seeds are then thought to amplify by the knock-on avalanche process [4]. Evidence for knock-on avalanche has been observed in startup REs [5], disruption REs [6] and rapid shutdown REs [7], although comparisons between RE growth rates and avalanche theory have not been done. A variety of experiments have attempted to use massive impurity injection to achieve collisional suppression of the REs generated during disruptions [7–10]. However, these experiments have achieved, at best, about 20% of the theoretically required electron density during the CQ, underlining the importance of confirming the theoretically predicted RE avalanche growth rate as a function of electric field and electron density.

Evidence that externally applied toroidal electric fields affect disruption REs was first seen in JT-60U [11]. Here, a more systematic study is performed: positive and negative toroidal electric fields are applied to position-stable RE beams and the resulting RE growth or decay rate is measured. The toroidal electric fields are applied with external ohmic electric field coils, giving fields from forward drive (to about $+1.5\,V\,m^{-1}$) to reversed drive (to about $-1.5\,V\,m^{-1}$). The drive is applied after the formation of 'RE plateau' currents (0.1–0.5 MA) in DIII-D created during rapid shutdown using mm-sized argon pellets containing 7 torr L (2.3×10^{20} atoms) of argon. We compare the DIII-D data with the predictions of an 'extended' avalanche theory and find qualitative agreement between observed trends in RE growth rates and theory; however, the addition of an apparent residual RE loss rate of order $10\,s^{-1}$ is required to obtain quantitative agreement between the data and the theory.

2. Overview of experiments

The experiments described here were performed on deuterium discharges in the DIII-D tokamak [12]. Typical pre-disruption plasma parameters were toroidal magnetic field $B_\phi = 2.1\,T$,

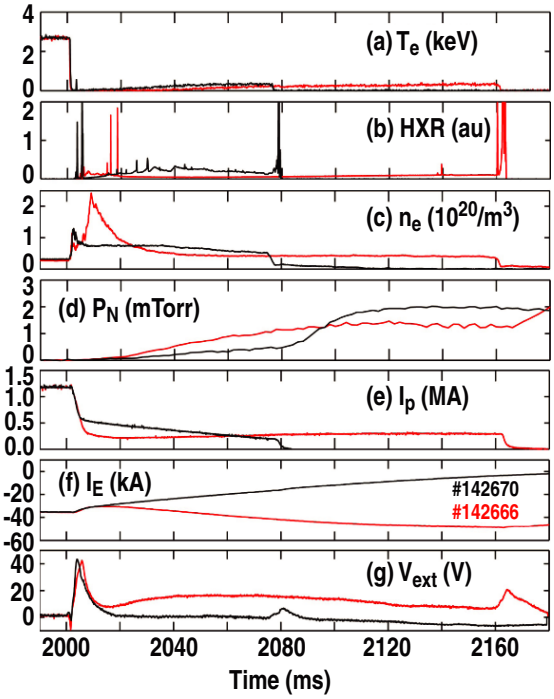

Figure 1. Time traces from two discharges differing primarily in the externally applied toroidal electric field direction during the RE plateau showing (*a*) electron temperature T_e, (*b*) HXR signals, (*c*) electron density n_e, (*d*) neutral pressure P_N, (*e*) plasma current I_p, (*f*) ohmic coil current I_E and (*g*) toroidal loop voltage measured outside the vacuum vessel V_{ext}.

electron density $n_e \approx 4 \times 10^{19}$ m^{-3} and electron temperature $T_e \approx 2.5$ keV. Most plasmas were run in a inner wall-limited, low-elongation ($\kappa \approx 1.3$–1.4) configuration; although several shots were run in a diverted, lower single null configuration. Heating was typically either ohmic only or ohmic plus electron cyclotron resonance heating (ECRH).

Time traces of plasma parameters from two discharges differing primarily in the externally applied toroidal electric field during the RE plateau are shown in figure 1. In one shot (red curve), a positive (driving) toroidal electric field is applied to the plasma; while in the other shot (black curve), a negative (braking) toroidal electric field is applied. The electric field is applied by ramping the ohmic coil current, I_E: rising ohmic coil current provides negative loop voltage, while a falling current applies positive loop voltage. The ohmic coil consists of two parallel-wired 61-turn air-core coils. Ohmic coil voltages of up to 900 V are used, giving maximum applied loop voltages of order $V_{app} \sim 15$ V and corresponding maximum applied electric fields of order $E_{app} \sim 1.5$ V m^{-1}. The initially quiescent plasma is shut down at time $t = 2000$ ms by rapid injection of a single small ($D \approx 2$ mm) argon pellet, causing a disruption thermal quench (TQ), as seen in core electron cyclotron emission (ECE), (figure 1(*a*)). The small nonzero signals seen for $t > 2010$ ms in ECE are thought to correspond to non-thermal RE emission. The observed slow rise in the RE ECE signal is not understood at present, but could be due to a variety of effects, such as radial motion of the RE beam, changes in RE energy, or changes in RE pitch angle; interpretive numerical modelling of the RE ECE signals is planned for future work. The extremely rapid TQ caused by the Ar pellet creates REs [13], as shown by the appearance of hard x-rays (HXRs) measured by scintillators [14], (figure 1(*b*)). Line-average electron density (figure 1(*c*)) is measured by a CO_2 interferometer, while average neutral pressure at the vessel wall (figure 1(*d*)) is measured by several ionization gauges at the vessel wall. Plasma current (figure 1(*e*)) is measured by coils inside the conducting wall surrounding the plasma; the plasma current in the RE plateau past the end of the initial current quench (CQ) $T > 2010$ ms is believed to be dominated by REs, since the decay time of thermal electron current in the CQ is known to be of order 5 ms [15]. The RE plateau typically lasts of order 100–200 ms before terminating suddenly. The cause of this final rapid loss of the RE beam is not fully understood, but appears to be due to the sudden loss of vertical control in at least some cases, possibly due to the RE current channel being narrower than the pre-disruption plasma. In this work, we will focus mostly on the middle of the RE plateau, where plasma position and measurable parameters (such as density and radiated power) are varying only slowly. The external toroidal loop voltage V_{ext} (figure 1(*g*)) is measured with a toroidal flux loop located in air just outside the conducting wall on the midplane on the high-field side of the plasma. It can be seen that the loop voltage created by the plasma during the CQ, of order 40 V, is larger than the plateau phase applied loop voltages of up to 15 V. The loop voltage values during the TQ in figure 1(*g*) are not necessarily thought to be accurate since the TQ time is shorter than the wall time and the flux loop is located outside the conducting wall.

3. RE avalanche theory

In this section, we discuss the behaviour of the RE plateau in the presence of an externally applied toroidal electric field E_{app} due to the ohmic coil ramp. The clear effect of the ohmic coil ramp direction on the RE current seen in figure 1 suggests that the RE avalanche growth rate ν_R is being affected: relativistic, mono-energetic (non-avalanching) REs would be expected to change energy (mass), but not velocity (current), due to changes in the toroidal loop voltage. Previous work [16] showed that the growth rate of RE current density J_R due to the knock-on avalanche mechanism is given approximately by $\nu_R = \bar{\nu}_E - \bar{\nu}_D$, where $\nu_R = J_R^{-1}\,\mathrm{d}J_R/\mathrm{d}t$, $\bar{\nu}_E = eE/(m_e c\bar{p})$ and $\bar{\nu}_D = eE_{crit}/(m_e c\bar{p})$, valid for $E - E_{crit} > 0$. Here, E is the in-plasma electric field, and $E_{crit} = e^3 n_{e,tot} \ln\Lambda(Z)/(4\pi\varepsilon_0^2 m_e c^2) = 0.0051 n_{e20} \ln\Lambda(Z)$ is the equivalent 'critical field' associated with the minimum collisional drag force (or stopping power) experienced by a fast electron passing through a medium of atomic number Z and total (free or bound) electronic density $n_{e,tot}$. We take p to be the electron momentum normalized by $m_e c$, and $\bar{p} = [3(Z+5)/\pi]^{1/2} \ln\Lambda(Z)$ is the mean value of p predicted for avalanching REs. For bound argon electrons, the Coulomb logarithm is $\ln\Lambda = 9.932$; while for bound carbon electrons, $\ln\Lambda = 10.9$ [17]; and for unbound (free) plasma electrons $\ln\Lambda = 19.2$. $\bar{p}$ is only weakly dependent on Z; for example, $\bar{p} = 46.5$ for drag on REs due to electrons bound to argon ($Z = 18$), $\bar{p} = 38.9$ for drag due to electrons bound to neon ($Z = 10$), and $\bar{p} = 46.3$ for drag due to free electrons.

Growth of RE current is self-limited by dropping loop voltage at the end of the CQ. After the end of the CQ, when production of new REs has ceased, the remaining discharge current is carried by REs. It can be shown analytically [18] that in this RE plateau phase, the RE distribution function becomes $f_R \sim \exp(-p/\bar{p})$, in close agreement with [16]. We show here for the first time what happens to the plateau-phase RE current in the braking case where $E - E_{\rm crit} < 0$. If a highly relativistic RE has normalized forward (parallel) momentum p at the beginning of the plateau phase $t = 0$, then at a later time t' it will have momentum p' given approximately by $p' = p + (e/mc)\int_0^{t'}(E - E_{\rm crit})\,{\rm d}t''$. Here, we are ignoring pitch-angle scattering collisions [19] relative to slowing-down collisions; this is expected to be valid for sufficiently relativistic electrons with $p > (Z + 1)$ [18, 20]. Substituting for p in the RE distribution function, we see that the shape of the distribution function remains unaltered. However, it possesses a time-dependent normalization such that when we evaluate the current density, $J_R = e\int vf\,{\rm d}p$, we obtain a 'symmetrical' RE rate formula $\nu_R = \bar{\nu}_E - \bar{\nu}_D$ *regardless of the sign of* $E - E_{\rm crit}$, i.e. this formula is valid for modelling the decay of plateau-phase RE currents when $E - E_{\rm crit} < 0$.

Currently, measurements of the internal in-plasma electric field E are not available. However, in the RE plateau phase, it is possible to derive an expression for the avalanche growth rate as a function of surface field $E_{\rm sur}$ to facilitate comparison between theory and experiment. During the RE plateau phase where transients on the wall time scale ($\tau_{\rm w} = L_{\rm ext}/R_{\rm w} \sim 10\,{\rm ms}$) have died away, and neglecting the small gap between the plasma edge and the wall, we expect the electric field outside the conducting wall $E_{\rm w}$ to be reasonably close to that measured at the surface of the plasma, $E_{\rm sur} \approx V_{\rm ext}/(2\pi R)$. For plateau-phase REs (zero Ohmic current) it can be shown from Poynting's Theorem [21] and a wall boundary condition [22] that the global RE current decay obeys $L_p\,{\rm d}I_R/{\rm d}t = -2\pi RE + L_{\rm ext}I_{\rm w}/\tau_{\rm w}$, where $L_p = \mu_0 R\ell_{\rm i}/2$ is the internal inductance of the RE channel, $\ell_{\rm i} = 1$–3 is the dimensionless self-inductance, $L_{\rm ext} \approx \mu_0 R[\log(8R/r_{\rm w}) - 2]$ is the external torus inductance in the circular large-aspect ratio approximation, and, for simplicity, we have assumed ${\rm d}L_p/{\rm d}t = 0$. A similar relation but neglecting wall currents was derived previously [23]. Since $R_{\rm w}I_{\rm w} = 2\pi RE_{\rm w}$, then by setting $E_{\rm w} \approx E_{\rm sur}$, we eliminate the in-plasma electric field E between the global relation and the symmetrical RE rate formula in order to express the RE growth/decay rate as a function of surface field, which can be used (rather than using the unknown internal field E) to compare against experimental data on ν_R:

$$\nu_R = \frac{\bar{\nu}_{\rm sur} - \bar{\nu}_D}{1 + \alpha_R}, \tag{1}$$

from which it also follows that

$$E - E_{\rm sur} = -\alpha_R(E - E_{\rm crit}), \tag{2}$$

where $\bar{\nu}_{\rm sur} = eE_{\rm sur}/(m_{\rm e}c\bar{p})$, $\alpha_R \equiv I_R\ell_{\rm i}/(\bar{p}I_{\rm A})$ and $I_{\rm A} = 4\pi m_{\rm e}c/(\mu_0 e) = 17\,{\rm kA}$ is the Alfvén current. The above relation tells us that the electric field always exceeds the surface field when the RE current is decaying, $E < E_{\rm crit}$. Furthermore, when the surface field is near zero (as is expected in the RE plateau phase if there are no externally applied electric fields),

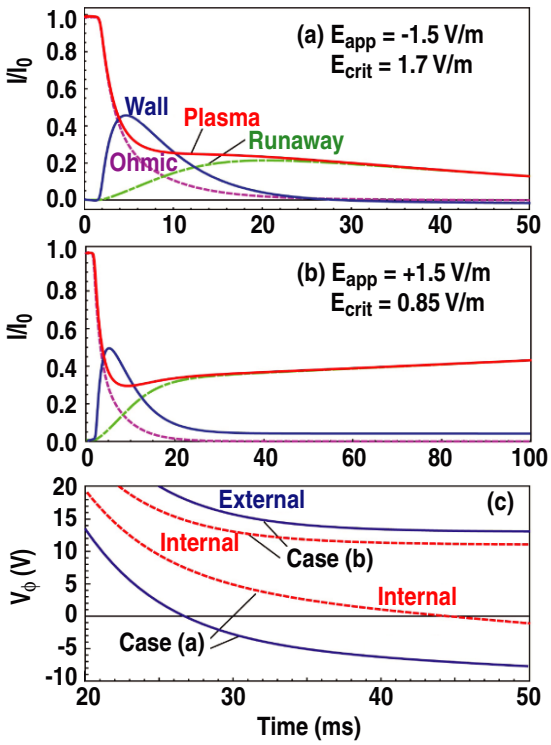

Figure 2. Time traces simulated using the coupled circuit model for showing plasma (runaway + ohmic) current, wall current, runaway current and ohmic current for different applied electric field (*a*) $E_{\rm app} = -1.5\,{\rm V\,m^{-1}}$ and (*b*) $E_{\rm app} = +1.5\,{\rm V\,m^{-1}}$; as well as (*c*) internal (to plasma) and external (to plasma) loop voltages for each case (*a*) and (*b*).

equation (2) shows that $E/E_{\rm crit} = 1/(1 + \alpha_R^{-1})$. In DIII-D, α_R is typically of order $\sim 1/2$, while for ITER it can be as high as $\sim$15, implying that only in high-current tokamaks like ITER will E be slightly less than $E_{\rm crit}$ during the RE plateau phase. For the same value of $E_{\rm crit}$, the RE decay rate according to equation (1) will be $\sim$10$\times$ slower in ITER than it is in DIII-D because of the much larger α_R.

Figure 2 shows simulations for DIII-D of two different shutdowns with different directions of $E_{\rm app}$, the externally applied toroidal field: $E_{\rm app} < E_{\rm crit}$ (damping), and $E_{\rm app} > E_{\rm crit}$ (amplifying). The simulations use a 0.5 D coupled circuit model with electron temperature prescribed to drop at $t = 0$ from $T_{\rm e} = 1\,{\rm keV}$ exponentially down on a TQ time scale of 0.65 ms to a floor of $T_{\rm e} = 2\,{\rm eV}$. The main elements of the coupled circuit model are described in [24]. Initial plasma current is taken to be $I_0 = 1.2\,{\rm MA}$ and initial RE seed current is taken to be 1% of this: $I_{\rm RE,0} = 12\,{\rm kA}$. The wall time is taken to be $\tau_{\rm w} = 7\,{\rm ms}$. The actual DIII-D toroidal wall time is believed to be closer to $\tau_{\rm w} \approx 10\,{\rm ms}$; however, a slightly shorter wall time is used here to approximately account for the gap between the plasma and the wall, which is not included in the 0.5 D model. The 0.5 D model also neglects changes in plasma self-inductance $\ell_{\rm i}$. Currently, best available data indicate $\ell_{\rm i} \approx 1$ before the TQ, $\ell_{\rm i} \approx 0.6$–1 during the CQ, and $\ell_{\rm i} \approx 1$–3 during the RE plateau. Here, since we are focused on the RE plateau, we use a higher average value $\ell_{\rm i} = 1.5$ for the purposes of the simulation. The critical fields are taken to be $E_{\rm crit} = 1.7\,{\rm V\,m^{-1}}$ in the braking case and $E_{\rm crit} = 0.85\,{\rm V\,m^{-1}}$

in the driving case; these values of E_{crit} are chosen to match experimentally observed ramp rates. Experimentally, these are reasonable assumptions, with the exception of E_{crit}: as will be discussed in section 5, values $E_{crit} \approx 0.1$–$0.3\,\mathrm{V\,m^{-1}}$ are theoretically expected for these experiments. The simulations therefore indicate an anomalously large E_{crit} or, alternatively, an additional RE loss term not included in the model and which is not constant between damping and amplifying cases. The simulations also indicate that (a) wall currents tend to be smaller than RE currents in the middle of the RE plateau; and (b) the difference between external and internal electric field is not negligible, even in the middle of the RE plateau.

4. RE plasma composition

Determining E_{crit} requires knowledge of the plasma atomic composition. The initial target plasma consists of dominantly D^+ ions plus about 2% C^{6+} ions, measured by charge-exchange recombination spectroscopy. During the rapid shutdown by Ar pellet injection, the target plasma experiences an influx of argon from the pellet, additional deuterium released during the TQ from the vessel walls [25, 26], and additional carbon sputtered from the vessel walls during the TQ [27]. In principle, both neutrals and ions could be present in the RE beam. Present estimates indicate that the atoms in the path of the RE beam consist largely of singly ionized ions: D^+ mixed with perhaps 20–30% Ar^+ and <1% C^+. Plasma visible spectra in figure 3 show (*a*) Ar II and C III emission for spectra integrating over the TQ; (*b*) disappearance of C III and strengthening of Ar II during the RE plateau; and (*c*) relatively weak Dα but strong C II during the RE plateau. Fitting to the line shapes in figure 3(*c*) gives $T_i \approx 1.6\,\mathrm{eV}$ for the C^+ ions and $T_N = 1.2\,\mathrm{eV}$ for the *D* neutrals. The disappearance of C III indicates that the RE plateau consists of dominantly singly ionized ions. A strong cooling of the bulk of the plasma electrons during the RE plateau is also consistent with UV survey spectra: figure 4 shows UV spectra taken during (*a*) the TQ, (*b*) the CQ and (*c*) the middle of the RE plateau. In the middle of the CQ, electron temperatures are expected to be of order $T_e \approx 3$–$5\,\mathrm{eV}$ [28]; consistent with this, significant line emission is observed from the plasma. However, during the RE plateau, line emission mostly disappears and the spectrum is dominated by a dim (∼10× weaker) continuum structure, possibly due to free-bound Ar I recombination radiation; this disappearance of UV line emission is consistent with a very low thermal electron temperature $T_e < 2\,\mathrm{eV}$.

The C^+ fraction can be estimated to be of order 0.01 or less from the C II (657.8 nm) line brightness. The thermal electron density $n_e \approx (5$–$15) \times 10^{19}\,\mathrm{m^{-3}}$ in the RE beam is known from interferometry. The RE density $n_R \approx (4$–$18) \times 10^{15}\,\mathrm{m^{-3}}$ can be estimated from the RE current and the RE beam radius *a*: $n_R ec \approx I_R/\pi a^2$, where the beam radius *a* is taken from equilibrium current reconstructions (EFIT). The thermal electron temperature in the RE plateau is expected to be well-equilibrated with the ion temperature, $T_e \approx T_i \approx 1.6\,\mathrm{eV}$. The RE temperature is assumed to be half-Maxwellian (from avalanche theory) with $T_R \approx 20\,\mathrm{MeV}$ (or $\tilde{p} \approx 40$) estimated from synchrotron emission brightness. Rates from [29] are used for the photon emission coefficient (PEC) of C II due to the thermal electrons. To estimate the PEC due to the REs,

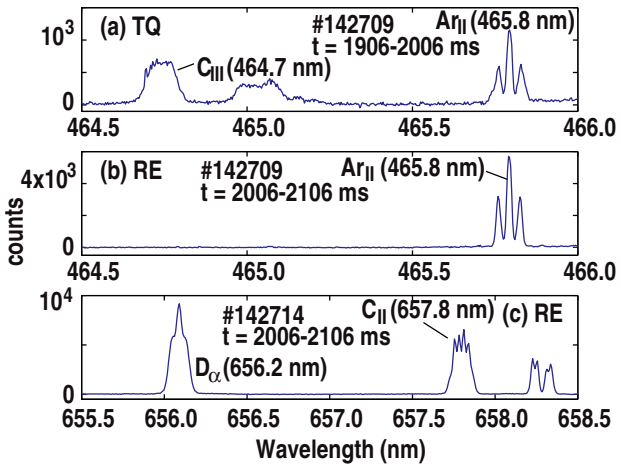

Figure 3. Central chord visible spectra of (*a*) Ar II and C III in the TQ, (*b*) Ar II in the RE plateau, and (*c*) Dα and C II in the RE plateau.

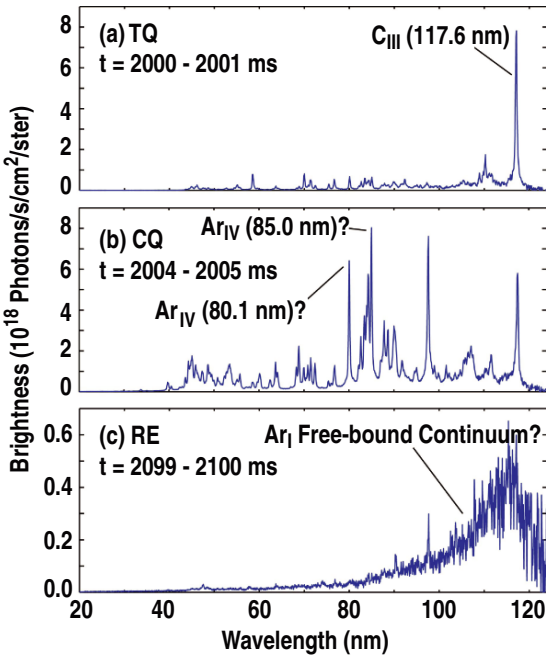

Figure 4. Central UV spectra at different times showing (*a*) the TQ, (*b*) the CQ and (*c*) the RE plateau phases.

we use the ionization cross sections for relativistic electrons on carbon [30] together with a photon efficiency $S/XB \approx 50$ estimated for C II (657.8 nm) in the limit of electron energies much higher than the C^+ ionization energy [29]. We estimate that the C II (657.8 nm) line brightness is dominantly (roughly 5× larger) due to thermal electron impact, rather than RE impact.

A similar spectroscopic estimate can also be made for the Ar^+ fraction, giving Ar^+ fractions of order $n_{Ar^+}/n_e \approx 0.2 \pm 0.1$. We use the thermal electron PEC for Ar II (465.8 nm) using ADAS calculations [29]. To estimate the PEC due to REs, we use the ionization cross section of Ar from relativistic electrons from [30], together with the correction for Ar^+ ionization from [31] and a photon efficiency $S/XB \approx 200$ estimated using the lower-energy Ar^+ ionization cross section compilation of [31]. We estimate that the Ar II (465.8 nm) line brightness is mostly

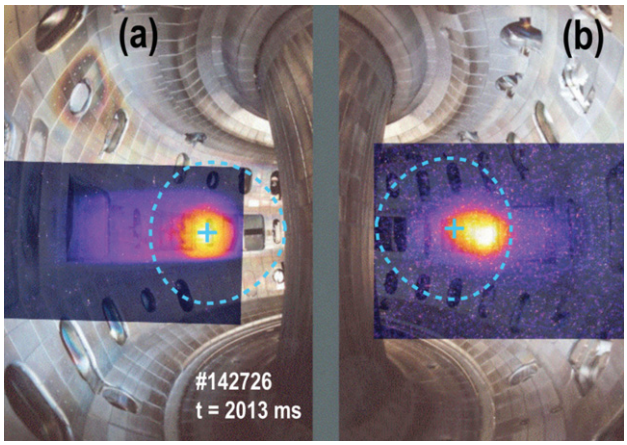

Figure 5. Visible emission images of the RE beam taken in (*a*) broadband emission looking in the counter-current direction and (*b*) the narrow band (901 nm) emission in the co-current direction and overlaid on photos of the vacuum vessel wall. Dashed lines are EFIT current density reconstructions showing the predicted separatrix location.

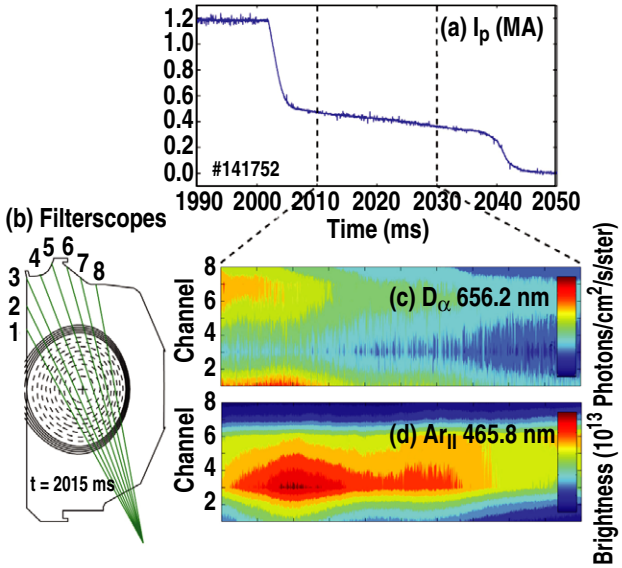

Figure 6. Spatial profile of visible emission from the RE beam showing (*a*) plasma current, (*b*) location of view chords, (*c*) spatial profile of Dα emission versus time, and (*d*) spatial profile of Ar II emission versus time.

(roughly 2× larger) due to thermal electron impact, rather than from RE impact.

An independent estimate of the RE beam argon ion content can be made from the neutral pressure measurement. Neutral pressures at the wall are measured to be of order $P_N \approx 1$ mTorr during the RE plateau. Assuming a low neutral temperature $T_N \approx 0.1$ eV, this corresponds to neutral density of order $n_N \approx 1.5 \times 10^{19}$ m^{-3}, i.e. perhaps (4–10)× lower than the thermal electron density in the plasma column. The argon pellet injects a known quantity of $N_{Ar} \approx 7$ Torr L ($= 2.3 \times 10^{20}$ atoms) of argon into the vacuum vessel. Vacuum system pumping times are long (seconds) and can be ignored here. We assume that the injected argon is conserved and is mixed uniformly through the background deuterium gas in the middle of the RE plateau, i.e. there is a constant atomic fraction $f_{Ar} = n_{Ar}/(n_{Ar} + n_D)$ throughout the plasma and neutral gas regions. We also assume that neutrals are largely excluded from the RE beam volume ($V_p \approx 10$ m^{-3}). Neutral temperature in the vacuum volume ($V_{vac} \approx 30$ m^{-3}) is expected to fall somewhere between the wall temperature 0.026 eV and the plasma ion temperature 1.5 eV; here, we simply assume $T_N \approx 0.1$ eV. Deuterons in the plasma are assumed to be all D^+ (not D_2^+ or D_3^+) and all D_2 (not D) in the vacuum region. With these assumptions, the total number of argon atoms in the vacuum vessel is

$$N_{Ar} \approx V_p n_e f_{Ar} + V_{vac} n_N \frac{2 f_{Ar}}{(1 + 2G_{Ar} f_{Ar} - f_{Ar})}, \qquad (3)$$

where $n_N = P_N/k_B T_N$ is the average vacuum region neutral density indicated by the pressure gauges and $G_{Ar} \approx 3$ is the gain of the pressure gauges for argon relative to deuterium. From equation (3), argon fractions $f_{Ar} \approx 0.3 \pm 0.1$, i.e. around 50% higher than the spectroscopic estimate, are obtained.

In the above calculations, we have used a simple two-zone (plasma region and neutral region) approximation. In reality, we expect there to be radial profiles of thermal electron temperature, thermal electron density, neutral density, etc. Evidence for a radial profile in RE beam parameters can be seen in visible images of the RE beam. Figure 5 shows a broadband image of a RE beam taken in the counter-current direction and a line-free narrow band (901 nm) image in the co-current direction. The counter-current image is expected to be dominated by line emission (Ar II, C II, and Dα), while the co-current image is expected to be dominated by RE synchrotron emission. Strong variation of both line emission and synchrotron emission across the beam profile can be seen, suggesting radial variation in both RE density and thermal electron density. Also, the plasma separatrix estimated from Grad–Shafranov equilibrium solutions constrained by external magnetic signals (EFIT) is overlayed on the images—it can be seen that the EFIT separatrix lies well outside much of the brightest emission region boundary. In contrast, preliminary analysis of the four available interferometer view chords suggests that the electron density profile extends to or beyond the EFIT separatrix boundary. This is supported by injections of small diagnostic pellets into the RE beams which have indicated that REs exist somewhat (∼10 cm) outside the EFIT separatrix [32]. These results thus suggest a strong radial variation in electron temperature (both thermal and RE). Here, we simply use a constant temperature model and one half the EFIT separatrix–separatrix path length for spectrometer optical path lengths and the full EFIT separatrix–separatrix path length for interferometer path lengths for the analysis described above.

The assumption used above that neutral argon is excluded from the RE beam is based on measured spatial profiles of Dα emission, which show some hollowing, as seen in (figure 6(*c*)). In contrast, ion line emission (from Ar II) (figure 6(*d*)) can be seen to be strongly centrally peaked about the central view channel #3, (figure 6(*b*)). Based on the Dα hollowing and on the significantly shorter ionization mean free path expected for Ar compared with D (because of the higher Ar mass and slower velocity), we expect neutral Ar to be mostly excluded from the centre of the RE beam. Basic calculations of the expected

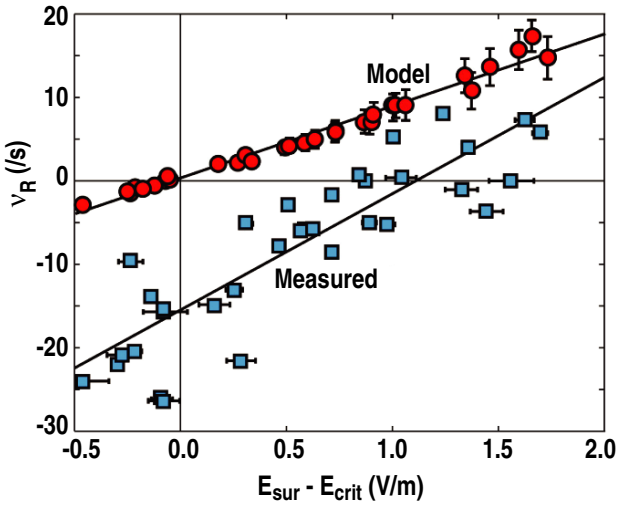

Figure 7. Measured (squares) and predicted (circles) RE growth rate ν_R as a function of the surface field minus critical field, $E_{sur} - E_{crit}$. Straight lines are linear fits to data.

argon neutral mean free path based on plasma parameters are not conclusive, however. For the mean free path of argon neutrals to electron-impact ionization we estimate values of order $\lambda_{ion} \approx 4$ m, with the ionization rate being dominated (by roughly 3×) by RE-impact, rather than thermal electron impact [30, 33]. For the mean free path of argon neutrals to forward momentum loss, we estimate values of order $\lambda_{mom} \approx 4$ cm, with the momentum loss rates due to D^+ impact and due to Ar^+ impact being roughly comparable [34, 35]. This gives a rough estimated effective argon ionization depth of order $\lambda_{ion,eff} = \sqrt{\lambda_{ion}\lambda_{mom}} \approx 30$ cm, which is comparable to the RE beam radius, so it is not clear from first principles if neutral argon penetration into the RE beam will be significant or not. We have ignored multiple ionization due to relativistic electron impact here, as this is not expected to be as large as single ionization.

5. Comparison of measured and calculated RE growth rate

In figure 7 we plot measured (squares) and predicted (circles) RE current growth rate ν_R as a function of surface field minus critical field, $E_{sur} - E_{crit}$. Each circle/square pair corresponds to the middle of the RE plateau in a single discharge. To calculate E_{crit}, we ignore carbon and take the average of the spectroscopic and pressure methods to calculate the Ar^+ fraction. The horizontal error bars on the squares in figure 7 reflect the range in E_{crit} obtained from the two different methods. These error bars are typically small even though the relative error in E_{crit} is quite large since typically $|E_{crit}| < |E_{sur}|$, i.e. $E_{crit} \approx 0.1$–0.3 V m^{-1} and $E_{sur} \approx -0.2$ to $+15$ V m^{-1}. The fact that these error bars are smaller than the scatter in the data suggests that the uncertainty in the plasma composition is not the dominant source of scatter in the data.

To use equation (1), the predicted growth rate as a function of $E_{sur} - E_{crit}$, the plasma self-inductance ℓ_i is required. Determining ℓ_i is challenging, since we do not have a direct measurement of the current distribution in the RE beam. In the pre-disruption plasma, $\ell_i \approx 1$; however, the current channel is then thought to expand, to $\ell_i < 1$ during the CQ and then re-compress to $\ell_i \geqslant 1$ during the RE plateau. Previous calculations have simply assumed $\ell_i \approx 2$ for plateau-phase RE beams [36]. In these experiments, EFIT gives a large range of values $\ell_i \approx 1$–3 during the RE plateau. Frequently, an increasing trend in ℓ_i is indicated, although it is not clear if this is real within the large scatter of the reconstructions. The EFIT Grad–Shafranov equilibrium does not necessarily describe the RE plateau accurately and even in the context of the standard Grad–Shafranov equilibrium, estimates of ℓ_i of nearly circular plasmas from external signals are not expected to be accurate. Here, we simply use $\ell_i \approx 2 \pm 1$ with vertical error bars shown on the theory points in figure 7 resulting from the uncertainly in ℓ_i.

Overall, even within the significant scatter of the data, it can be seen that there is a clear ramp up or down of the RE current in response to changes in the surface field E_{sur}. Also, the trend of the experimental and theory curves appear to be in reasonable agreement, but with an offset of order -10 to -15 s^{-1}. The origin of this offset is not clear at present. It is likely that neutral Ar is penetrating at least partially into the RE beam; this would be consistent with the mean free path calculations presented above, although not with the observation of hollow Dα emission of (figure 6(*c*)). Penetration of argon neutrals into the RE beam is expected to have an effect of order $E_{crit} \approx 0.1$–0.3 V m^{-1} or less, however, since neutral densities are expected to be lower than plasma densities by 4–10× (or of order 1–3× if we use lowest possible value of neutral temperature $T_N = 0.026$ eV instead of $T_N = 0.1$ eV). Assuming a pure Ar plasma with a 100% room-temperature Ar neutral penetration into the plasma nearly removes the offset of figure 7; however, this scenario appears highly unlikely based on present data.

Another possible explanation for the observed offset is shrinking of the current channel. As discussed above, we have assumed a constant value of plasma self-inductance $\ell_i \approx 2 \pm 1$ in our analysis of the data. However, because of this large uncertainty in ℓ_i, we cannot rule out the possibility that the RE current profile is consistently shrinking at a rate of order $(d\ell_i/dt)/\ell_i \approx 10$ s^{-1}, thus causing the observed secular drop in plasma current I_p (by conservation of magnetic flux $L_p I_p$).

The favoured explanation for the offset at present is radial transport of REs to the wall by some type of steady-state (as opposed to intermittent) transport. Clear signatures of intermittent instabilities dumping REs to the wall are seen by narrow spikes on the HXR signals, (figure 1(*b*)); however, these instabilities do not appear to correlate with increased loss in plateau RE current. The effective radial RE diffusion coefficient $D_{\perp R}$ corresponding to the observed steady RE loss rate of -10 s^{-1} is quite modest, $D_{\perp R} \sim 0.4$ m^2 s^{-1}. This finding is similar to previous observations in JT-60U, where steady (non-intermittent) plateau-phase RE current decay was observed even with positive loop voltage [37, 38]. In the JT-60U experiments, toroidal field ripple scatter and/or secondary synchrotron radiation of the scattered electrons were suggested as possible plateau-phase RE loss mechanisms [11]. Numerical simulations have shown that RE losses to the wall can be quite significant in the presence of magnetic field errors; these errors were presumed to result from overlapping internal MHD modes [39], applied magnetic fields [40], or magnetic

turbulence of indeterminate origin [23, 41]. Drift-orbit loss of energetic REs to the outer midplane has also been considered as a possible steady-state RE loss mechanism [42]. The radial drift-orbit shift of REs is of order $\Delta R_{\mathrm{RE}} \approx qp_{\parallel}/eB$, giving $\Delta R_{\mathrm{RE}} \approx 7\,\mathrm{cm}$ for 20 MeV electrons in a $B = 2\,\mathrm{T}$ field. This is consistent with the radial shift in the synchrotron spot seen in figure 6(*b*) and is significant when compared with the RE beam radius of order 20 cm. However, the apparent systematic trend in the background loss term seen in figure 7 (from about $-8\,\mathrm{s}^{-1}$ for largest values of surface field down to perhaps $-17\,\mathrm{s}^{-1}$ for smallest values of surface field) does not appear consistent with drift-orbit loss, i.e. larger loop voltages would be expected to increase $p_{||}$ thus increasing RE drift-orbit loss to the wall.

In the analysis presented here, we have ignored RE formation due to Dreicer [1] or hot tail [2] mechanisms. This is expected to be a valid assumption, since in the middle of the RE plateau, the background plasma temperature and toroidal electric field are both low. For example, using thermal electron temperature $T_{\mathrm{e}} = 1.6\,\mathrm{eV}$ and density $n_{\mathrm{e}} = 10^{20}\,\mathrm{m}^{-3}$, we arrive at a Dreicer field $E_{\mathrm{D}} \approx E_{\mathrm{crit}}(0.5\,\mathrm{MeV}/T_{\mathrm{e}}) \approx 3 \times 10^4\,\mathrm{V\,m}^{-1}$. For typical mid-RE plateau electric fields $E \approx 1\,\mathrm{V\,m}^{-1}$, the Dreicer RE growth rate $\nu_{\mathrm{D}} \propto \exp(-E_{\mathrm{D}}/4E)$ can thus be ignored. Hot tail formation gives an enhancement over Dreicer RE formation if the thermal plasma electron–electron collision frequency ν_{ee} is slow compared with the cooling rate of the electron temperature. In the middle of the plateau, however, we expect $\nu_{\mathrm{ee}} \approx 10^9\,\mathrm{s}^{-1}$, which is fast compared with typical plasma evolution time scales of order $0.1\,\mathrm{s}^{-1}$, so we expect hot tail RE formation to be negligible.

6. Summary

In summary, clear changes in the current of plateau-phase RE beams are seen in response to applied toroidal electric fields. Comparisons between measured current growth/decay rates and predictions of avalanche theory suggest the presence of a background loss of REs at a rate of order $-10\,\mathrm{s}^{-1}$. Currently, this loss is hypothesized to be due to radial transport of REs to the wall, although other possible explanations for the apparent background loss (such as shrinking of the current channel) cannot be ruled out yet. Future experiments and analysis will attempt to quantify radial loss of REs and obtain improve estimates of the in-plasma toroidal electric field. Future experiments will also attempt to obtain improved data on the composition and radial profile of the RE beam. For example, there is a discrepancy at present between the apparent poor neutral pumping of the RE beam (as seen by the high neutral pressures measured at the wall) and the apparent lack of neutral penetration (as seen by the hollow Dα profile); this discrepancy might be due to a large sink of ions at the edge of the RE beam—either due to recombination or due to recycling on the wall. These and future related studies are expected to assist in developing system requirements for safe rampdown or dissipation of RE beams in future large tokamaks such as ITER.

Acknowledgments

This work was supported by the US Department of Energy under DE-FG02-07ER54917, DE-FG02-05ER54809, DE-AC05-00OR22725, DE-FC02-04ER54698, DE-FG02-95ER54309 and DE-FG03-97ER54415. The originating developer of ADAS is the JET Joint Undertaking.

References

[1] Dreicer H. 1960 *Phys. Rev.* **117** 329
[2] Smith H.M. and Verwichte E. 2008 *Phys. Plasmas* **15** 072502
[3] Savrukhin P.V. 2006 *Plasma Phys. Control. Fusion* **48** B201
[4] Sokolov A.Yu. 1979 *JETP Lett.* **29** 218
[5] Jaspers R., Finken K.H., Mank G., Hoenen F., Boedo J.A., Cardozo N.J.L. and Schuller F.C. 1993 *Nucl. Fusion* **33** 1775
[6] Gill R.D., Alper B., de Barr M., Hender T.C., Johnson M.F., Riccardo V. and contributors to the EFDA-JET Work programme 2002 *Nucl. Fusion* **42** 1039
[7] Bozhenkov S.A. *et al* and the TEXTOR team 2008 *Plasma Phys. Control. Fusion* **50** 105007
[8] Hollmann E.M. *et al* 2010 *Phys. Plasmas* **17** 056117
[9] Commaux N., Baylor L.R., Jernigan T.C., Hollmann E.M., Parks P.B., Humphreys D.A., Wesley J.C. and Yu J.H. 2010 *Nucl. Fusion* **50** 112001
[10] Pautasso G. *et al* and the ASDEX Upgrade Team 2009 *Plasma Phys. Control. Fusion* **51** 124056
[11] Yoshino R. and Tokuda S. 2000 *Nucl. Fusion* **40** 1293
[12] Luxon J.L. 2002 *Nucl. Fusion* **42** 614
[13] Evans T.E. *et al* 1999 *Proc. of the IAEA 17th Int. Fusion Energy Conf. (Yokahama, Japan, 19–24 October 1998)* vol 3 p 847 http://www-pub.iaea.org/MTCD/Publications/PDF/csp_001c/html/iaeacn69.htm
[14] James A.N., Hollmann E.M. and Tynan G.R. 2010 *Rev. Sci. Instrum.* **81** 10E306
[15] Humphreys D.A. and Whyte D.G. 2000 *Phys. Plasmas* **7** 4057
[16] Rosenbluth M.N. and Putvinski S.V. 1997 *Nucl. Fusion* **37** 1355
[17] Evans R.D. 1955 *The Atomic Nucleus* (New York: McGraw-Hill)
[18] Parks P.B., Rosenbluth M.N. and Putvinski S.V. 1999 *Phys. Plasmas* **6** 2523
[19] Mosher D. 1975 *Phys. Fluids* **18** 846
[20] Fussmann G. 1979 *Nucl. Fusion* **19** 327
[21] Ejima S., Callis R.W., Luxon J., Stambaugh R.D., Taylor T.S. and Wesley J.C. 1982 *Nucl. Fusion* **22** 1313
[22] Parks P.B., Wu W. and APS 2007 Theoretical progress on runaway electron suppression by massive particle injection *49th Annual Meeting of the Division of Plasma Physics (Orlando, FL, USA, 12–16 November 2007)* (American Physical Society) abstract #JP8.109 (http://meetings.aps.org/ Meeting/DPP07/Event/70549)
[23] Helander P., Eriksson L.G. and Andersson F. 2002 *Plasma Phys. Control. Fusion* **44** B247
[24] Hollmann E.M., Parks P.B. and Scott H.A. 2008 *Control. Plasma Phys.* **48** 260
[25] Hollmann E.M. *et al* 2009 *J. Nucl. Mater.* **390–391** 597
[26] Philipps V. *et al* 2009 *J. Nucl. Mater.* **390–391** 478
[27] Hollmann E.M. *et al* 2003 *Phys. Plasmas* **10** 2863
[28] Hollmann E.M. *et al* 2008 *Nucl. Fusion* **48** 115007
[29] Sommers H.P. *et al* 2002 *Plasma Phys. Control. Fusion* **44** B323 and http://www.adas.ac.uk/
[30] Rieke F.F. and Prepejchal W. 1972 *Phys. Rev.* A **6** 1507
[31] Salop A. 1974 *Phys. Rev.* A **9** 2496
[32] James A.N. *et al* 2011 *Pellet interaction with runaway electrons J. Nucl. Mater* at press
[33] Raju G.G. 2006 *Gaseous Electronics: Theory and Practice* (Boca Raton, FL: CRC Press)
[34] Krstic P.S. and Schultz D.R. 1999 *Phys. Rev.* A **60** 2118
[35] Nichols B.J. and Witteborn F.C. 1966 Measurement of resonant charge-exchange cross-sections in nitrogen and

argon between 0.5 and 17 eV *NASA Technical Note* D-3265
[36] ITER physics expert group on disruptions, plasma control, and MHD 1999 *Nucl. Fusion* **39** 2251
[37] Kawano Y. *et al* 2002 *Fusion Sci. Technol.* **42** 298
[38] Yoshino R., Tokuda S. and Kawano Y. 1999 *Nucl. Fusion* **39** 151
[39] Izzo V.A. *et al* 2011 *Nucl. Fusion* **51** 063032
[40] Papp G., Drevlak M., Fulop T. and Helander P. 2011 *Nucl. Fusion* **51** 043004
[41] Sanchez R., Martin-Solis J.R. and Esposito B. 2003 *Comput. Phys. Commun.* **156** 95
[42] Guan X., Hong Q. and Fisch N. 2010 *Phys. Plasmas* **17** 092502